CHIN. PHYS. LETT. Vol. 27, No. 2 (2010) 027203

Competition between Radiative Power and Dissipation Power in the Refrigeration Process in Oxide Multifilms *

ZHANG Li-Li(张莉莉), HU Chun-Lian(胡春莲), WANG Can(王灿), LÜ Hui-Bin(吕惠宾), HAN Peng(韩鹏), YANG Guo-Zhen(杨国桢), JIN Kui-Juan(金奎娟)**

Beijing National Laboratory for Condensed Matter Physics, Institute of Physics, Chinese Academy of Sciences, Beijing 100190

(Received 24 July 2009)

The maximum refrigeration power dependence on the doping density in the p-$BaTiO_3$/$BaTiO_3$/$SrTiO_3$/$BaTiO_3$/n-$BaTiO_3$ system and in the p-AlGaAs/AlGaAs/GaAs/AlGaAs/n-AlGaAs system is obtained respectively based on the opto-thermionic refrigeration model. The results show that the maximum refrigeration power in the p-$BaTiO_3$/$BaTiO_3$/$SrTiO_3$/$BaTiO_3$/n-$BaTiO_3$ system increases dramatically with the increase of doping density from 1.0×10^{18} cm^{-3} to 5.0×10^{19} cm^{-3} while that in the p-AlGaAs/AlGaAs/GaAs/AlGaAs/n-AlGaAs system is nearly a constant. It is found that the different Auger coefficients and the competition between radiative power and dissipation power lead to the different behavior of the maximum refrigeration power dependence on the doping density of the two systems.

PACS: 72. 20. Pa, 78. 60. Fi DOI: 10.1088/0256-307X/27/2/027203

As an important perovskite oxide material, strontium titanate ($SrTiO_3$) has been attracted great attention.[1–3] Many heterostructures based on $SrTiO_3$ such as $La_{0.8}Sr_{0.2}MnO_3$/Nb-doped $SrTiO_3$ p-n junctions, $BaTiO_3$/$SrTiO_3$ superlattices, $SrTiO_3$/Si field effect transistors and $La_{0.67}Sr_{0.33}MnO_3$/$SrTiO_3$/$La_{0.67}Sr_{0.33}MnO_3$ tunnel junctions have been fabricated with atomically smooth interfaces.[3–7] With the development of electronic and optoelectronic devices based on $SrTiO_3$, cooling becomes an important and new issue for this material.

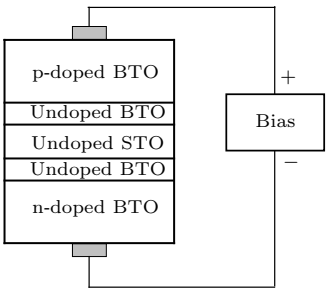

Fig. 1. Schematic illustration of the structure of the p-BTO/BTO/STO/BTO/n-BTO opto-thermionic refrigeration system.

Combining the traditional thermionic refrigeration[8] with laser refrigeration,[9–12] opto-thermionic refrigeration in semiconductor heterostructures has been proposed by Mal'Shukov *et al.*[13] Based on this method, hot electrons and holes are emitted into the well region by the thermionic emission process. In the well region, these hot carriers recombine to emit light and the heat is extracted by the photons. There exists dissipation heat resulting from all recombination processes. When the dissipation power $Q_{\rm dis}$ is smaller than the light emission power $Q_{\rm rad}$, refrigeration is realized.

Although great attention has been paid to the opto-thermionic refrigeration in the GaAs based heterostructures,[13,14] little research work has been carried out with the opto-thermionic refrigeration process in the perovskite oxide heterostructures. In this Letter, we present a detailed theoretical study on the opto-thermionic refrigeration system of p-$BaTiO_3$/$BaTiO_3$/$SrTiO_3$/$BaTiO_3$/n-$BaTiO_3$. The schematic illustration of the system is plotted in Fig. 1. The lengths of p-doped and n-doped $BaTiO_3$ (BTO) regions, BTO spacers and $SrTiO_3$(STO) well are 200 nm, 20 nm and 40 nm, respectively.

To obtain the refrigeration power, the distribution of carrier densities is calculated based on the drift-diffusion model. In the calculation, the Richardson current[15] is used as the boundary condition at the interfaces between BTO and STO. The method for the calculation of electron and hole concentrations in the quantum well is the same as that in the system of p-AlGaAs/AlGaAs/GaAs/AlGaAs/n-AlGaAs, which was described in detail in our previous work.[14] The refrigeration power $Q_{\rm refrig}$ is

$$\begin{aligned} Q_{\rm refrig} &= Q_{\rm rad} - Q_{\rm dis} \\ &= E_{\rm g-well} \int_{\rm well} R_{\rm rad}(x)dx \\ &\quad - V_{\rm bias} \int_{\rm well} \left(R_{\rm rad}(x) + R_{\rm Aug}(x)\right) dx, \end{aligned} \tag{1}$$

where $E_{\rm g-well}$ is the band gap of STO, $V_{\rm bias}$ is the

*Supported by the National Natural Science Foundation of China and the National Basic Research Program of China
**To whom correspondence should be addressed. Email: kjjin@aphy.iphy.ac.cn

applied bias voltage, $R_{\rm rad}(x)$ and $R_{\rm Aug}(x)$ are the radiative and Auger recombination rates, respectively. The recombination rates are written as[16,17]

$$R_{\rm rad}(x) = B(n(x)p(x) - n_i^2), \tag{2}$$

$$R_{\rm Aug}(x) = C(n(x) + p(x))(n(x)p(x) - n_i^2), \tag{3}$$

with B, C, $n(x)$, $p(x)$ and n_i denoting the radiative recombination coefficient, Auger coefficient, electron density, hole density and the intrinsic carrier density, respectively. The parameters used in the calculation are listed in Table 1.

Table 1. Material parameters used in the calculation (Refs. [2,18–23]).

	GaAs	STO
$E_{\rm g-well}$ (eV)	1.42	3.2
Radiative coefficient ($\rm cm^3 s^{-1}$)	1.9×10^{-10}	1.0×10^{-11}
Auger coefficient ($\rm cm^6 s^{-1}$)	3.0×10^{-30}	1.7×10^{-32}
Electron mobility ($\rm cmV^{-1}s^{-1}$)	8000	33
Hole mobility ($\rm cmV^{-1}s^{-1}$)	400	10

Based on the opto-thermionic model, the refrigeration power dependence on the bias voltage in the heterostructures of p-BTO/BTO/STO/BTO/n-BTO and p-AlGaAs/AlGaAs/GaAs/AlGaAs/n-AlGaAs is obtained, respectively. The maximum refrigeration power $Q_{\rm max}$ in both the heterostructures is at $V_{\rm max} = 3.06\,\rm V$ and $V_{\rm max} = 1.36\,\rm V$, respectively.

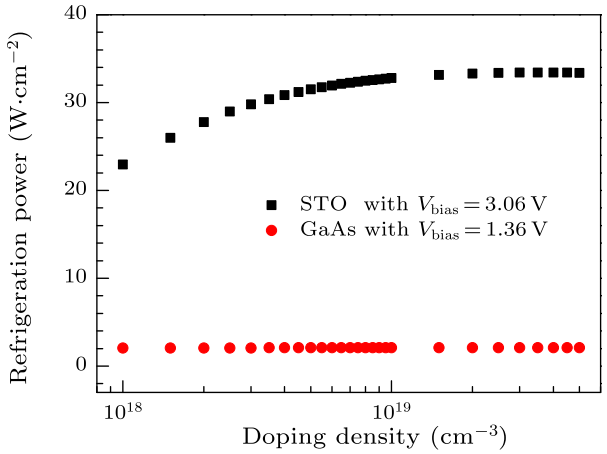

Fig. 2. The maximum refrigeration power versus the doping density for (a) the p-BTO/BTO/STO/BTO/n-BTO system at $V_{\rm max} = 3.06\,\rm V$ and for (b) the p-AlGaAs/AlGaAs/GaAs/AlGaAs/n-AlGaAs system at $V_{\rm max} = 1.36\,\rm V$, respectively.

The maximum refrigeration power $Q_{\rm max}$ versus the doping density for the p-BTO/BTO/STO/BTO/n-BTO and the p-AlGaAs/AlGaAs/GaAs/AlGaAs/n-AlGaAs system is plotted in Fig. 2, respectively. The donor density in the n-doped region is set to be equal to the acceptor density in the p-doped region for simplicity, which is $N_{\rm donor} = N_{\rm acceptor} = N_{\rm imp}$.

As shown in Fig. 2, the maximum refrigeration power $Q_{\rm max}$ in the p-BTO/BTO/STO/BTO/n-BTO system increases from $22.96\,\rm W\,cm^{-2}$ to $33.40\,\rm W\,cm^{-2}$ with the doping density $N_{\rm imp}$ increasing from $1.0 \times 10^{18}\,\rm cm^{-3}$ to $5.0 \times 10^{19}\,\rm cm^{-3}$. In the p-AlGaAs/AlGaAs/GaAs/AlGaAs/n-AlGaAs system, $Q_{\rm max}$ increases from $2.08\,\rm W\,cm^{-2}$ to $2.09\,\rm W\,cm^{-2}$ with the increase of the doping density from $1.0 \times 10^{18}\,\rm cm^{-3}$ to $5.0 \times 10^{19}\,\rm cm^{-3}$. It is clearly seen that the maximum refrigeration power $Q_{\rm max}$ in the p-BTO/BTO/STO/BTO/n-BTO system increases nearly 50% while in the p-AlGaAs/AlGaAs/GaAs/AlGaAs/n-AlGaAs system it varies slightly with the doping density $N_{\rm imp}$ increasing from $1.0 \times 10^{18}\,\rm cm^{-3}$ to $5.0 \times 10^{19}\,\rm cm^{-3}$.

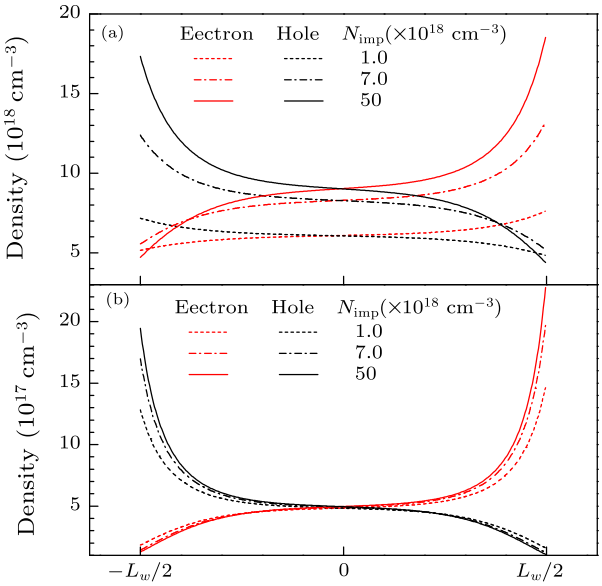

Fig. 3. Spatial distribution of electron and hole densities in the well region with $N_{\rm imp} = 1.0 \times 10^{18}\,\rm cm^{-3}$, $7.0 \times 10^{18}\,\rm cm^{-3}$, and $5.0 \times 10^{19}\,\rm cm^{-3}$ for (a) the p-BTO/BTO/STO/BTO/n-BTO system at $V_{\rm max} = 3.06\,\rm V$ and for (b) the p-AlGaAs/AlGaAs/GaAs/AlGaAs/n-AlGaAs system at $V_{\rm max} = 1.36\,\rm V$, respectively. L_W denotes the width of the well region.

To explain the different behavior of the maximum refrigeration power dependence on the doping density in the two systems, the spatial distribution of carriers in the well region with $N_{\rm imp} = 1.0 \times 10^{18}\,\rm cm^{-3}$, $7.0 \times 10^{18}\,\rm cm^{-3}$ and $5.0 \times 10^{19}\,\rm cm^{-3}$ for the p-BTO/BTO/STO/BTO/n-BTO system at $V_{\rm max}$ (3.06 V) and for the p-AlGaAs/AlGaAs/GaAs/AlGaAs/n-AlGaAs system at $V_{\rm max}$ (1.36 V) is plotted in Figs. 3(a) and 3(b), respectively. As shown in this figure, the carrier densities in the well region increases with the increase of the doping density at $V_{\rm max}$.

The radiative power and the dissipation power versus the doping density in the p-BTO/BTO/STO/BTO/n-BTO system at $V_{\rm max}$(3.06 V) and the p-AlGaAs/AlGaAs/GaAs/AlGaAs/n-AlGaAs system at $V_{\rm max}$(1.36 V) are plotted in Figs. 4(a) and 4(b), respectively. It can be seen that in the p-BTO/BTO/STO/BTO/n-

BTO system the radiative power and the dissipation power increase dramatically with the increase of the doping density while in the p-AlGaAs/AlGaAs/GaAs/AlGaAs/n-AlGaAs opto-thermionic system they are nearly constants. This should be the reason that the maximum refrigeration power $Q_{\max}$ in the p-BTO/BTO/STO/BTO/n-BTO system increases nearly 50% and that in the p-AlGaAs/AlGaAs/GaAs/AlGaAs/n-AlGaAs system varies slightly with the doping density increase. From Eqs. (2) and (3), it can be seen that the Auger recombination rate is more sensitive to the carrier densities than the radiative recombination rate. Therefore, in the p-BTO/BTO/STO/BTO/n-BTO system, due to the small Auger coefficient of STO, the increasing rate of $Q_{\rm rad}$ is much larger than that of $Q_{\rm dis}$ with the doping density $N_{\rm imp}$ increasing from $1.0\times10^{18}\,{\rm cm}^{-3}$ to $5.0\times10^{19}\,{\rm cm}^{-3}$. On the other hand, in the p-AlGaAs/AlGaAs/GaAs/AlGaAs/n-AlGaAs system, owing to the large Auger coefficient of GaAs, the increasing rate of $Q_{\rm rad}$ is nearly the same as that of $Q_{\rm dis}$ with the increase of the doping density $N_{\rm imp}$ from $1.0\times10^{18}\,{\rm cm}^{-3}$ to $5.0\times10^{19}\,{\rm cm}^{-3}$. The competition between radiative power and dissipation power results in the small increase of the maximum refrigeration power. In conclusion, the different behavior of the maximum opto-thermionic refrigeration power dependence on the doping density of the two systems is due to the different Auger coefficients of the two systems and the competition between radiative power and dissipation power.

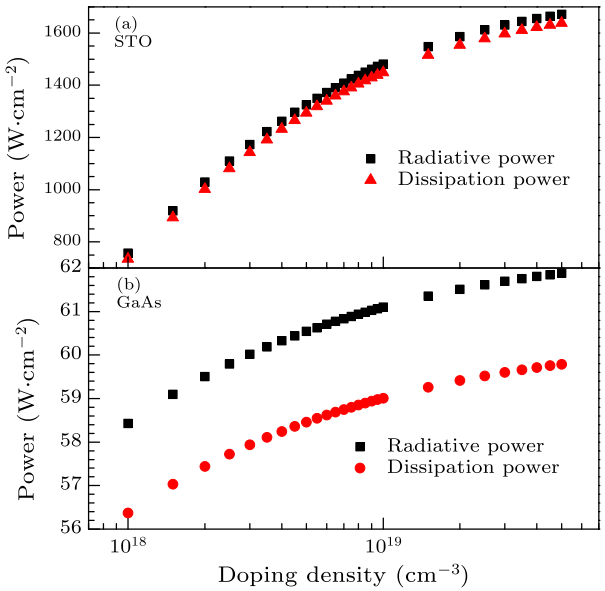

Fig. 4. Radiative power and dissipation power versus the doping density in (a) the p-BTO/BTO/STO/BTO/n-BTO system at $V_{\max} = 3.06\,{\rm V}$ and in (b) the p-AlGaAs/AlGaAs/GaAs/AlGaAs/n-AlGaAs system at $V_{\max} = 1.36\,{\rm V}$, respectively.

In summary, the maximum refrigeration power dependence on the doping density is obtained in the p-BTO/BTO/STO/BTO/n-BTO and the p-AlGaAs/AlGaAs/GaAs/AlGaAs/n-AlGaAs systems, respectively. It is found that the refrigeration power in the p-BTO/BTO/STO/BTO/n-BTO system is much larger than that in the p-AlGaAs/AlGaAs/GaAs/AlGaAs/n-AlGaAs system. The maximum refrigeration power in the p-BTO/BTO/STO/BTO/n-BTO system increases more than $10\,{\rm W\,cm}^{-2}$ while that in the p-AlGaAs/AlGaAs/GaAs/AlGaAs/n-AlGaAs system is nearly a constant with the doping density increasing from $1.0\times10^{18}\,{\rm cm}^{-3}$ to $5.0\times10^{19}\,{\rm cm}^{-3}$. It is found that the different Auger coefficients and the competition between radiative power and dissipation power lead to the different behavior of the maximum refrigeration power dependence on the doping density of the two systems.

At the end of study, we should mention that the oxygen vacancy of perovskite oxides should play an important role in opto-thermionic refrigeration. Further study on the refrigeration power including the nonradiative recombination resulting from the oxygen vacancy is expected, as well as experimental investigations.

References

[1] Szot K, Speier W, Bihlmayer G and Waser R 2006 *Nature Mater.* **5** 312
[2] Bellingeri E, Pellegrino L, Marré D, Pallecchi I and Siri A S 2003 *J. Appl. Phys.* **94** 5976
[3] Yang G Z, Lu H B, Chen F, Zhao T and Chen Z H 2001 *J. Crystal Growth* **227–228** 929
[4] Wang C C, Liu G Z, He M and Lu H B 2008 *Appl. Phys. Lett.* **92** 052905
[5] Wang N, Lu H B et al 1999 *Appl. Phys. Lett.* **75** 3464
[6] Eisenbeiser K et al 2000 *Appl. Phys. Lett.* **76** 1324
[7] Wertz E T and Li Q 2007 *Appl. Phys. Lett.* **90** 142506
[8] Mahan G D 1994 *J. Appl. Phys.* **76** 1362
[9] Pringsheim P 1929 *Z. Phys.* **57** 739
[10] Jia Y H, Zhong B, Ji X M and Yin J P 2008 *Chin. Phys. Lett.* **25** 85
[11] Ding K and Zeng Y P 2008 *Chin. Phys. Lett.* **25** 1878
[12] Jia Y H et al 2008 *Chin. Phys. Lett.* **25** 3779
[13] Mal'shukov A G and Chao K A 2001 *Phys. Rev. Lett.* **86** 5570
[14] Han P, Jin K J et al 2006 *J. Appl. Phys.* **99** 074504
[15] Horio K and Yanai H 1990 *IEEE Trans. Electron Devices* **37** 1093
[16] Sze S M 1981 *Physics of Semiconductor Devices* (New York: Wiley)
[17] Abakumov V N, Perel V I and Yassievich I N 1991 *Nonradiative Recombination in Semiconductors* (Amsterdam: North-Holland)
[18] Šik J, Schubert M et al 2000 *Appl. Phys. Lett.* **76** 2859
[19] Strauss U, Rüle W W and Köler K 1993 *Appl. Phys. Lett.* **62** 55
[20] Rubano A, Paparo D et al 2007 *Phys. Rev.* B **76** 125115
[21] Yasuda H and Kanemitsu Y 2008 *Phys. Rev.* B **77** 193202
[22] Takeda K et al 1985 *Phys. Rev.* B **32** 1101
[23] Liu L F, Guo H Z et al 2005 *J. Appl. Phys.* **97** 054102